

Superwide-band negative refraction of a symmetrical E-shaped metamaterial with two electromagnetic resonances

Changchun Yan,^{1,2} Yiping Cui,^{1,*} Qiong Wang,¹ and Shichuang Zhuo¹

¹Advanced Photonics Center, School of Electronic Science and Engineering, Southeast University, Nanjing 210096, China

²School of Physics and Electronic Engineering, Xuzhou Normal University, Xuzhou 221116, China

(Received 21 December 2007; published 6 May 2008)

A symmetrical E-shaped metamaterial is investigated in this paper. Numerical simulations disclose the two electromagnetic resonances and the superwide negative-refractive band of this structure. The distributions of the induced current in the E-shaped copper wires show that these two electromagnetic resonances originate from the current flowing in the different C-shaped rings. The retrieved negative-refractive band is superwide, and the negative refraction with high transmission occurs in the different bands. The metamaterial with two or even more electromagnetic resonances offers an opportunity for the realization of wide-band negative refraction.

DOI: [10.1103/PhysRevE.77.056604](https://doi.org/10.1103/PhysRevE.77.056604)

PACS number(s): 41.20.Jb, 78.20.Ci, 73.20.Mf, 42.25.Bs

A notable metamaterial, a left-handed material (LHM) (with simultaneously negative permittivity ϵ and negative permeability μ), was discussed by Veselago [1] in 1968, following that work by Pendry *et al.* [2–4]. However, the LHM has attracted increasing interest until the demonstration of the LHM by Smith *et al.* [5,6]. This LHM made use of an array of split-ring resonator (SRR) elements to achieve negative effective permeability, and an array of continuous wires to obtain negative effective permittivity, a simultaneous combination resulting in the LHM [6–8]. To date, there have also been a few other ways towards the realization of the LHM, including pairs of metallic nanorods [9], fishnet structures [10–12], and ultrathin waveguides [13], of which frequency regions have ranged from microwave to visible spectrum in the past several years. As far as the SRR-wire method is concerned, it has been developed as many forms, such as an Ω -shaped method [14], an S-shaped method [15], an H-shaped method [16], etc. [17,18]. Nevertheless, in each method, the electromagnetic resonance peak is usually only one, and the negative-refractive band is also narrow, lying roughly around the electromagnetic resonance frequency. This greatly restricts practical applications for the LHMs.

In this paper, however, we propose a configuration in which each unit cell consists of two symmetrical E-shaped wires. The simulated S-parameter responses exhibit two electromagnetic resonance phenomena, originating from the different resonances among E-shaped rings. The complex refractive index n , wave impedance z , effective permittivity ϵ , and effective permeability μ are retrieved from the S parameters. It is found that the negative-refractive band is superwide, lying roughly below the electromagnetic resonance with higher frequency. This offers a good idea of obtaining LHMs with wide-frequency bands.

As shown in Figs. 1(a) and 1(b), the configuration we consider here is a periodic copper array, in which every unit cell consists of two symmetrical E-shaped wires [as outlined by the rectangular dashed line in Fig. 1(a)]. The metamaterial

extends infinitely along the x and y directions, while its thickness along the z direction is only one unit cell. This unit cell is cubic. A substrate of FR4 (permittivity $\epsilon=4.4$, loss tangent of 0.02) is assumed. Two symmetrical E-shaped wires are positioned on the substrate, modeling the structures typically produced by lithographic circuit board techniques. Other parts in this unit cell are occupied by vacuum. All dimensions are displayed in the caption under Fig. 1. As for geometry, the E-shaped metamaterial can be regarded as a combination of symmetrical metallic C-shaped resonators (note that only one unit cell contains several C-shaped reso-

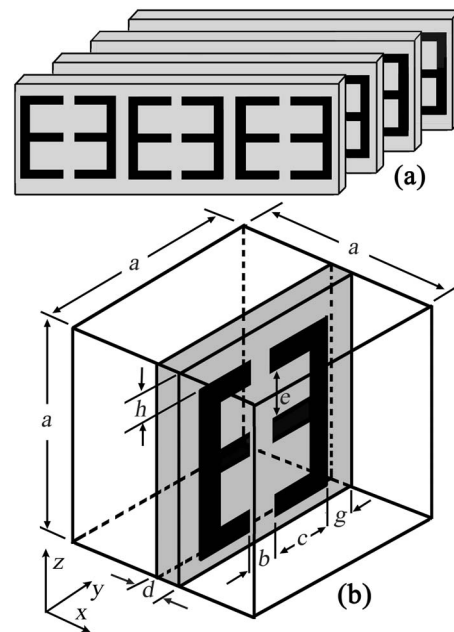


FIG. 1. (a) Schematic for the array of an E-shaped metamaterial. The rectangular dashed line outlines the E shape. (b) A unit cell with geometric dimensions $a=2.5$ mm, $b=0.2$ mm, $c=1$ mm, $d=0.1$ mm, $e=0.7$ mm, $h=0.25$ mm, and, $g=0.15$ mm. The metal (copper) is 0.2 mm in width and 0.01 mm in thickness. The propagation of the polarized electromagnetic wave is along the z axis, and the electric field and the magnetic field are in the y and x directions, respectively.

*Author to whom correspondence should be addressed. cyp@seu.edu.cn

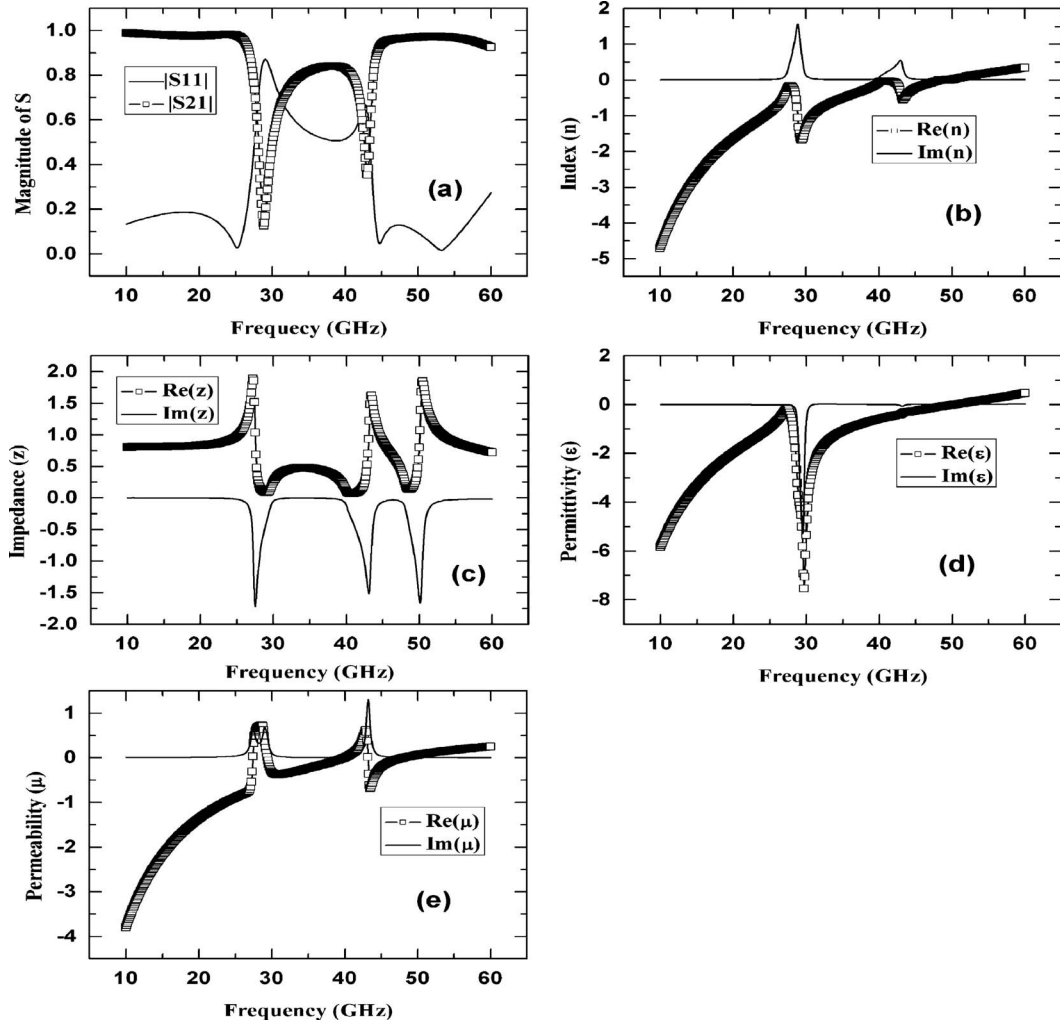


FIG. 2. (a) Magnitude of the simulated S parameters for the unit cell in Fig. 1(b); (b) retrieved refractive index; (c) retrieved impedance; (d) retrieved permittivity; (e) retrieved permeability.

nators) and continuous wires. The metamaterials with ring resonators generally generate magnetic oscillation with above gigahertz frequencies [19,20]. Below plasma frequency, the continuous-wire metamaterials also yield negative effective permittivity [3]. Therefore, this symmetrical E-shaped metamaterial can exhibit negative refraction in a certain frequency band, which can be demonstrated below the simulations.

A High Frequency Structure Simulator, a commercial electromagnetic mode solver, is used in our simulations. To verify the simulations and the retrieved electromagnetic parameters, we first investigated a copper SRR-wire unit cell, in which the copper SRR and wire are set on opposite sides of a substrate. The scales, wave ports and boundary conditions in the unit cell are the same as those in Fig. 2 in Ref. [21]. (Note that the structure is symmetrical along electromagnetic wave direction, leading to $S_{11}=S_{22}$ among S parameters.) Our simulated S-parameter responses are in agreement with those in Fig. 3 in Ref. [21]. Based on Eqs. (9), (10), and (4) in Ref. [21], namely,

$$n = \frac{1}{kd} \cos^{-1} \left[\frac{1}{2S_{21}} (1 - S_{11}^2 + S_{21}^2) \right], \quad (1)$$

$$z = \sqrt{\frac{(1 + S_{11})^2 - S_{21}^2}{(1 - S_{11})^2 - S_{21}^2}}, \quad (2)$$

$$\varepsilon = n/z, \quad \mu = nz, \quad (3)$$

we can retrieve values for the complex refractive index n , wave impedance z , effective permittivity ε , and effective permeability μ . The frequency responses we obtain are completely coincident with those in Ref. [21].

Because the structural symmetry of the E-shaped unit cell in this work is similar to that of the SRR-wire unit cell, the same method can be employed to investigate our designed structure. To excite the negative magnetic response of the C resonators as well as the negative electric response of the continuous wires, the incident electromagnetic waves are polarized with the magnetic field perpendicular to the C-resonator plane ($\mathbf{H} \parallel x$ axis) and the electric field parallel to the y axis ($\mathbf{E} \parallel y$ axis). Consequently, the propagation direction (wave vector \mathbf{K}) is along the z axis. The two wave ports are set in the planes perpendicular to the z axis. The perfect

magnetic and electric boundaries (corresponding to the boundaries perpendicular to the x and y axes, respectively) are applied.

In our calculations, we require a maximum deviation of 0.25% on the magnitude of scattering parameters between iterations. Eleven iterations lead to a meshing of 4912 tetrahedrons, with a 0.17% error of scattering parameter magnitude between the two last iterations.

Both the S parameters and the retrieved material parameters are described in Fig. 2. Figure 2(a) shows the magnitude of the computed S parameters. It is evident that the two electromagnetic resonances appear in this structure. (The reason for the two electromagnetic resonances will be discussed below.) The retrieved index in Fig. 2(b) confirms the negative-refractive band lying between 10 GHz (f_1) and 47.8 GHz (f_2) in the calculated frequency range. We suppose that center frequency f_0 and ratio γ are defined as $(f_1 + f_2)/2$ and $(f_2 - f_1)/f_0$, respectively. With this geometry we find the ratio $\gamma > 1.3$. This ratio is much larger than that in the past work (often $\gamma < 0.5$) [12,15,16,21–23], which indicates that this metamaterial exhibits broadband negative-refractive response. Additionally, $-n_1/n_2 > 1$ is satisfied below 27.3 GHz, between 29.1 GHz and 39.9 GHz, and between 43.2 GHz and 48 GHz, which implies high transmission with low loss in these frequency bands. Here n_1 and n_2 are the real and imaginary parts of the refractive index. Therefore, this metamaterial could have potential for practical applications. In addition, the retrieved impedance, the retrieved permittivity and the retrieved permeability are shown in Figs. 2(c)–2(e), respectively. As shown in Figs. 2(d) and 2(e), we can obtain negative real parts of permittivity and permeability [i.e., $\text{Re}(\epsilon) < 0$ and $\text{Re}(\mu) < 0$ simultaneously] below 27.3 GHz, between 29.5 GHz and 39.9 GHz, and between 43.3 GHz and 48.1 GHz, differing from the band of the negative-refractive index. Negative $\text{Re}(n)$ is achieved throughout as the condition $\epsilon_1\mu_2 + \mu_1\epsilon_2 < 0$ is satisfied [22,23], where $\epsilon = \epsilon_1 + i\epsilon_2$ and $\mu = \mu_1 + i\mu_2$. Moreover, Fig. 2(e) shows the strong magnetic resonances [$\text{Re}(\mu) = -0.38$ and $\text{Re}(\mu) = -0.69$] occurring around frequency of 30.9 GHz and 43.5 GHz, respectively. However, the magnetic absorption is weaker [$\text{Im}(\mu) = 0.032$ and $\text{Im}(\mu) = 0.715$ at the corresponding frequencies]. Around the lower magnetic-resonance frequency, there is also an electric resonance [see Fig. 2(d)], which indicates the existence of an LC resonance circuit. However, an electric resonance can hardly rise around the higher magnetic-resonance frequency. This means that there is mainly magnetic resonance producing around this frequency. From Figs. 2(e) and 2(d), we can also see that $\text{Re}(\mu)$ and $\text{Re}(\epsilon)$ are negative and characterized by analogous frequency responses in the lower frequency band. The reason lies in the complicated interaction of several C-shaped rings, resulting in magnetic plasma response similar to electric plasma response in this frequency band. These similar plasma forms are also in agreement with those presented in many papers [24,25].

Next, to explain the two-resonance phenomenon, the distributions of induced current in the E-shaped copper wires are shown near the corresponding frequencies. Figure 3(a) shows clearly that the lower-frequency resonance peak mainly originates from the induced current flowing in the

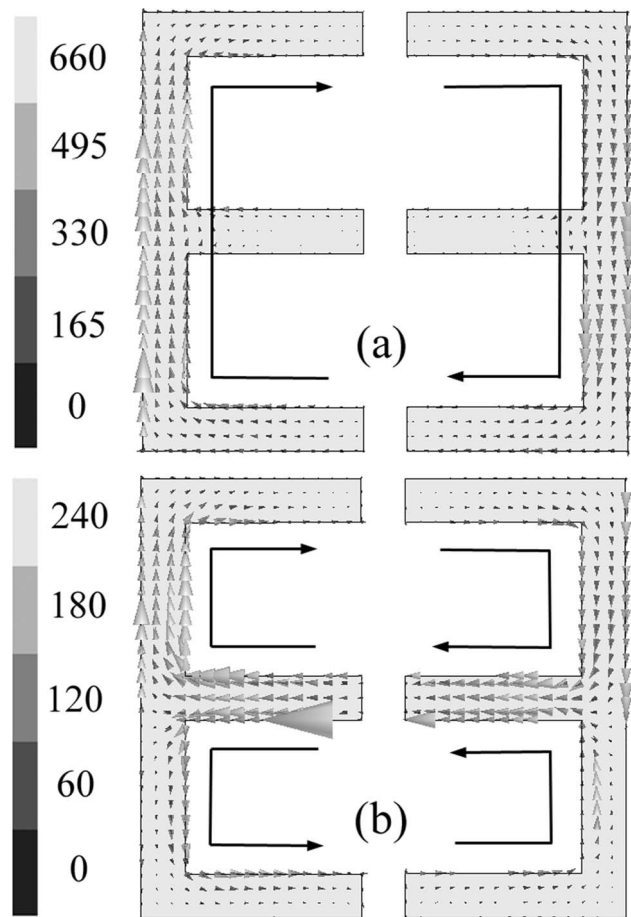


FIG. 3. Distributions of induced current in the E-shaped copper wires at the frequencies of (a) 29 GHz and (b) 43 GHz.

two bigger C-shaped rings [see the two curves with arrows in Fig. 3(a)]. Around another resonance peak, however, the induced current flowing in the four smaller C-shaped rings primarily results in the resonance [see the four curves with arrows in Fig. 3(b)]. It is also obvious that the resonance frequency should be higher because of the current induced in the smaller C-shaped rings, while the current in the bigger ones naturally leads to the lower resonance frequency.

In conclusion, a symmetrical E-shaped metamaterial has been investigated in this paper. Numerical simulations exhibit the two-resonance phenomenon and the superwide negative-refractive band of this structure. The simulated S-parameter responses display two electromagnetic resonances, and the distributions of the induced current in the E-shaped copper wires show clearly that the two electromagnetic resonances originate from the induced current in the different C-shaped rings. The complex refractive index n , wave impedance z , effective permittivity ϵ , and effective permeability μ have been retrieved from the S parameters. The strong magnetic resonances are found around the frequencies of 30.9 GHz and 43.5 GHz, and the negative-refractive band is superwide, lying below 47.8 GHz. Furthermore, the negative-refractive band with high transmission with low loss occurs below 27.3 GHz, between 29.1 GHz and 39.9 GHz, and between 43.2 GHz and 48 GHz, which is

helpful for practical applications. At the same time, $\text{Re}(\mu)$ and $\text{Re}(\epsilon)$ are negative and characterized by analogous frequency responses in the lower frequency band. More importantly, if a metamaterial has a characteristic of two or even

more electromagnetic resonances, this metamaterial has potential for wider-band negative refraction, which presents a new strategy for obtaining LHMs with wide-frequency bands.

-
- [1] V. G. Veselago, *Sov. Phys. Usp.* **10**, 509 (1968).
- [2] J. B. Pendry, A. J. Holden, D. J. Robbins, and W. J. Stewart, *IEEE Trans. Microwave Theory Tech.* **47**, 2075 (1999).
- [3] J. B. Pendry, A. J. Holden, W. J. Stewart, and I. Youngs, *Phys. Rev. Lett.* **76**, 4773 (1996).
- [4] J. B. Pendry, *Phys. Rev. Lett.* **85**, 3966 (2000).
- [5] D. R. Smith, W. J. Padilla, D. C. Vier, S. C. Nemat-Nasser, and S. Schultz, *Phys. Rev. Lett.* **84**, 4184 (2000).
- [6] R. A. Shelby, D. R. Smith, and S. Schultz, *Science* **292**, 77 (2001).
- [7] M. Bayindir, K. Aydin, E. Ozbay, P. Markos, and C. M. Soukoulis, *Appl. Phys. Lett.* **81**, 120 (2002).
- [8] R. B. Gregor, C. G. Parazzoli, K. Li, and M. H. Tanielian, *Appl. Phys. Lett.* **82**, 2356 (2003).
- [9] V. M. Shalaev, W. S. Cai, U. K. Chettiar, H. K. Yuan, A. K. Sarychev, V. P. Drachev, and A. V. Kildishev, *Opt. Lett.* **30**, 3356 (2005).
- [10] S. Zhang, W. J. Fan, N. C. Panoiu, K. J. Malloy, R. M. Osgood, and S. R. J. Brueck, *Phys. Rev. Lett.* **95**, 137404 (2005).
- [11] G. Dolling, C. Enkrich, M. Wegener, C. M. Soukoulis, and S. Linden, *Science* **312**, 892 (2006).
- [12] G. Dolling, M. Wegener, C. M. Soukoulis, and S. Linden, *Opt. Lett.* **32**, 53 (2007).
- [13] H. J. Lezec, J. A. Dionne, and H. A. Atwater, *Science* **316**, 430 (2007).
- [14] J. Huangfu, L. Ran, H. Chen, X.-M. Zhang, K. Chen, T. M. Grzegorzcyk, and J. A. Kong, *Appl. Phys. Lett.* **84**, 1537 (2004).
- [15] H. Chen, L. Ran, J. Huangfu, X. Zhang, K. Chen, T. M. Grzegorzcyk, and J. A. Kong, *Phys. Rev. E* **70**, 057605 (2004).
- [16] J. Zhou, T. Koschny, L. Zhang, G. Tuttle, and C. M. Soukoulis, *Appl. Phys. Lett.* **88**, 221103 (2006).
- [17] S. G. Mao, S. L. Chen, and C. W. Huang, *IEEE Trans. Microwave Theory Tech.* **53**, 1515 (2005).
- [18] B. Hu, H. Wen, Y. Leng, and W. J. Wen, *Appl. Phys. Lett.* **87**, 201114 (2005).
- [19] C. Enkrich, M. Wegener, S. Linden, S. Burger, L. Zschiedrich, F. Schmidt, J. F. Zhou, Th. Koschny, and C. M. Soukoulis, *Phys. Rev. Lett.* **95**, 203901 (2005).
- [20] A. K. Sarychev, G. Shvets, and V. M. Shalaev, *Phys. Rev. E* **73**, 036609 (2006).
- [21] D. R. Smith, D. C. Vier, T. Koschny, and C. M. Soukoulis, *Phys. Rev. E* **71**, 036617 (2005).
- [22] S. Zhang, W. Fan, N. C. Panoiu, K. J. Malloy, R. M. Osgood, and S. R. J. Brueck, *Phys. Rev. Lett.* **95**, 137404 (2005).
- [23] F. M. Wang, H. Liu, T. Li, Z. G. Dong, S. N. Zhu, and X. Zhang, *Phys. Rev. E* **75**, 016604 (2007).
- [24] C. Liu, C. C. Yan, H. Chen, and Y. Liu, *Appl. Phys. Lett.* **88**, 231102 (2006).
- [25] S. A. Cummer, *Appl. Phys. Lett.* **82**, 2008 (2003).